Small Solar Panels Can Drastically Reduce the Carbon Footprint of Radio Access Networks

Ana Paula Couto da Silva[1], Daniela Renga[2], Michela Meo[2], Marco Ajmone Marsan[2,3]
1 - Computer Science Department, Universidade Federal de Minas Gerais - Brazil
2 - Electronics and Telecommunications Department, Politecnico di Torino - Italy
3 - IMDEA Networks Institute - Spain
ana.coutosilva@dcc.ufmg.br, daniela.renga@polito.it, michela.meo@polito.it, marco.ajmone@polito.it

***Abstract*—The limited power requirements of new generations of base stations make the use of renewable energy sources, solar in particular, extremely attractive for mobile network operators. Exploiting solar energy implies a reduction of the network operation cost as well as of the carbon footprint of radio access networks, but previous research works indicate that the area of the solar panels that are necessary to power a standard macro BS is large, so large to make the solar panel deployment problematic, especially within urban areas.**

In this paper we use a modeling approach based on Markov reward processes to investigate the possibility of combining small area solar panels with a connection to the power grid to run a macro base station. By so doing, it is possible to increase the amount of renewable energy used to run a radio access network, while also reducing the cost incurred by the network operator to power its base stations.

We assume that energy is drawn from the power grid only when needed to keep the BS operational, or during the night, that corresponds to the period with lowest electricity price. This has advantages in terms of both cost and carbon footprint.

We show that solar panels of the order of 1-2 kW peak, i.e., with a surface of about 5-10 m^2, combined with limited capacity energy storage (of the order of 10-15 kWh, corresponding to about 3-5 car batteries), and a smart energy management policy, can lead to an effective exploitation of renewable energy.

***Index Terms*—Radio access network, Base station, Energy consumption, Renewable energy, Green networking, Solar panel**

I. Introduction

Green networking has been a hot research topic for the last 15 years, since the seminal paper by Gupta and Singh [1] raised the awareness of the networking research community on the increasing amount of energy necessary to run the Internet. The attention devoted by researchers to green networking is the result of a multidimensional concern, evolving around three main axes: i) the energy density required to run networks in large metropolitan areas, ii) the carbon footprint of the networking domain, iii) the energy contribution to the operational expenditures (OPEX) of network operators (NOs)

A number of international research projects have been devoted to the issue of energy efficiency in networking over the last decade, such as EARTH [2], ECONET [3], TREND [4], and GreenTouch [5]. Many approaches to a more parsimonious use of energy have been developed within those projects, mostly related to the introduction of sleep modes (or low-power-idle modes) in the operation of network equipment (see for example [6]–[8] for a survey of research in the field). At the same time, networking equipment manufacturers managed to develop new generations of devices with an increased attention to power consumption.

In the particular case of radio access networks (RANs), the most energy-hungry components are base stations (BSs), that largely contribute to the OPEX incurred by mobile NOs (MNOs). Consider for example that China Mobile, the worlds largest MNO, with a few million installed BSs, pays an energy bill corresponding to a consumption of several tens TWh per year [9]. While BS models of the last decade consumed up to 3.5 kW, the latest models need less than 1 kW, and expert predictions forecast peak power consumption around 700 W [10].

The expected reduction of the energy intake of BSs spurred investigations of the feasibility of using renewable energy sources (RES), solar radiation in particular, to power BSs in locations where the power grid is not available or not reliable, or just where the cost of connecting the BS to the power grid is high. Exploiting RES means using "green energy" rather than the "brown energy" available from the power grid, which is mostly generated by burning fossil fuels. The results of these studies generally indicate that the area of solar panels that are necessary to power a BS is large [11]; so large to make the solar panel deployment problematic, especially within urban areas.

In this paper we use a modeling approach based on Markov reward processes to investigate the possibility of combining small area solar panels with a connection to the power grid, with the objective of increasing the amount of green energy used to run the BS, and of reducing the MNO OPEX due to energy. Brown energy is drawn from the power grid only when needed to keep the BS running, or during the night, that corresponds to the period with lowest consumption, hence with lowest price. This has advantages both in terms of cost and in terms of carbon footprint, since the excess energy that is produced in periods of very low consumption may be wasted.

The key contributions of this paper are the following.

We apply for the first time a Markov reward model to the investigation of the energy consumption of a BS connected to a solar panel, an energy storage and the power grid. The reward describes as a continuous variable the battery charge, that in previous studies was shown to be the most critical

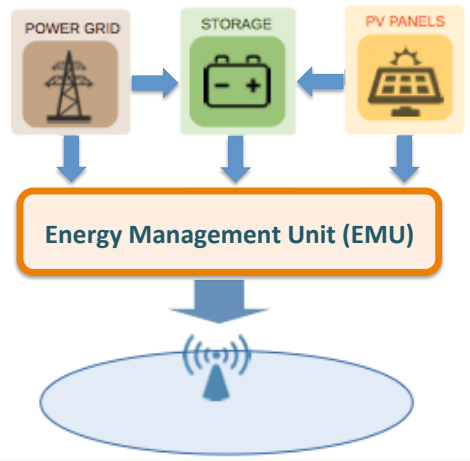

Fig. 1: The considered BS power system.

system element as regards quantization [12].

We investigate the difference in behavior and performance of the BS power system over the 4 seasons by considering a location at 45 degrees North (Torino, Italy), where the impact of seasons is significant.

We show that small area solar panels (of the order of 1-2 kW peak, i.e., about 5-10 m^2) combined with limited capacity energy storage (of the order of 10-15 kWh, corresponding to about 3-5 lead acid, 12 V, 120 Ah, car batteries), and a smart energy management policy, can lead to an effective exploitation of renewable energy. That is, can lead to systems where the probability of the battery being empty remains low, so that the amount of energy acquired from the grid is small, and the probability of the battery being full does not grow too high, so that the amount of energy produced by the solar panel that is wasted because it cannot be stored in the battery is small.

The rest of this paper is structured as follows. Section II describes the system setup that we consider in this paper. Section III illustrates the Markov reward model developed for the considered scenario. Section IV presents and discusses numerical results. Section V describes some previous work related to the content of this paper, and Section VI concludes the paper.

II. System Description

We consider one macro BS, equipped with a solar panel and an energy storage unit. The BS power system is controlled by an energy management unit (EMU) that is connected to the BS, the solar panel, the energy storage (that we will simply call "battery") and the power grid. The considered setup is illustrated in Figure 1.

During periods of energy production of the solar panel, the EMU uses the generated power to run the BS. If the generated power is less than necessary, power is drained from the battery. If the generated power is more than necessary, the excess power is directed to the battery. If the power generated by the panel is insufficient to run the BS and the battery is depleted, power is acquired from the grid.

Power can also be drawn from the grid in periods of low energy cost to recharge the battery for later use.

The energy entering and exiting the battery is subject to losses, that we assume equal to 15% at both the battery input and output.

A. Energy consumption model

In order to model the BS power consumption we use the approach that has become standard in the field, and that was defined in the FP7 project EARTH [2]. The power needed to operate a macro BS can be expressed as:

$$P_{in} = N_{TX} \,.\, (P_0 + \Delta_p \,.\, P_{out}), \;\; 0 < P_{out} < P_{max} \qquad (1)$$

where N_{TX} is the number of BS transceivers, P_{max} represents the maximum radio frequency output power at full load for one transceiver, P_0 corresponds to the fixed power consumption for one transceiver when the radio frequency output power is zero, and Δ_p is the slope of the load-dependent power consumption. P_{out} is derived as:

$$P_{out} = \rho \,.\, P_{max}, \;\; 0 \leq \rho \leq 1 \qquad (2)$$

where ρ denotes the instantaneous normalized BS load.

The power consumption of a LTE macro BS with 3 sectors, 2x2 MIMO, operating over 20 MHz has been derived considering the forecast consumption of BSs in year 2020 [10], according to which the typical minimum and maximum values of the power consumption P_{in} are 114.5 W and 817.1 W, respectively.

The daily variation of the parameter ρ is defined by the BS traffic profiles. We use real traces provided by an Italian mobile network operator [13]. The daily traffic patterns measured in a cell in a business area (BA) and in a cell in a residential area (RA), during week-day (wd) and week-end (we), are provided in Figure 2, setting the maximum observed load equal to the maximum load that can be carried by the BS (i.e., $\rho = 1$).

B. Renewable energy production model

The parameters of the energy production stochastic model are derived from two traces available in the Solar Radiation Data (SoDa) website for the city of Torino, Italy.

The first (long-term) trace contains daily average irradiance values, collected from January 1st 1985 to December 31st 2005. The second (short-term) trace contains hourly average irradiance values, collected from February 1st 2004 to December 31st 2006. This data is provided by NASA (USA) and MINES Paris Tech/Armines (France), considering global radiation in the horizontal plane [14].

We aggregate the available long-term and short-term data into 4 season-based sets: Winter months, from December to February (90 or 91 days per year); Spring, from March to May

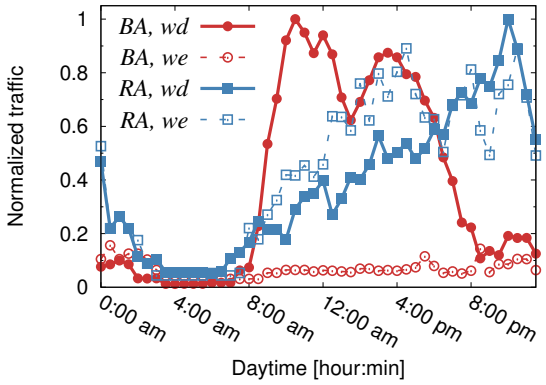

Fig. 2: Week-day (wd) and week-end (we) traffic loads in a business (BA) and residential (RA) area.

(92 days); Summer, from June to August (92 days); Autumn, from September to November (91 days).

For each season, from the long-term irradiance data we generate the average daily energy production of a 1 kW peak solar panel, and we define an energy production histogram by applying an equal-range discretization. That is, we first divide the total production range (difference between the maximum and minimum daily average productions over the 21-year period in the considered season) into 5 ranges of equal size, as in [12], and we compute the frequency (probability) of each interval. This procedure defines *day-types*, i.e., distinguishes between 5 types of days based on the average daily production. The same data are also used to obtain the probabilities that a day-type j follows a day-type i, with $i, j \in [1, \cdots, 5]$.

Given the day-type, using the short-term irradiance data we also model the hourly energy production. We split the energy produced at a given hour of a given day-type into ranges of 100 Wh each, and we build a histogram for all samples of a given day-type in a given season. The number of possible intervals of size 100 Wh varies according to season and it is denoted by $N_L^{(S)}$ for season S, so that the maximum production in season S is $100 \cdot N_L^{(S)}$ Wh.

Figure 3 reports the average hourly irradiance profiles for each season. As expected, irradiance is highest in summer and lowest in winter, and values of irradiance in spring are significantly higher than in autumn. Note also the difference among useful irradiance hours in the different seasons; while in summer irradiance values are higher than zero from about 5 am to 9 pm, in winter the useful interval is from 7 am to 6 pm. The average daily peaks vary from 333 W/m^2 in winter to 791 W/m^2 in summer.

In Figure 4 we disaggregate the seasonal data, and we report for each season the average irradiance profiles observed for each day-type. Day-types with the highest irradiance (day-types 5) have similar profiles in spring and summer; a higher irradiance variability among day-type profiles is however observed in spring with respect to summer. Conversely, day-types with the lowest values of irradiance (day-types 1) show similar average profiles in autumn and winter, with a higher irradiance variability among day-type profiles in autumn.

Figure 5 further disaggregates the irradiance data and displays the daily irradiance profiles observed for each day-type and each season. We can see that in summer (and to a lower extent also in spring) day-type 5 corresponds to patterns of high irradiance values, with limited variability from day to day. For day-types corresponding to intermediate to low solar irradiance, a higher variability from day to day can be observed, as well as a more relevant intra-day variation. For day-type 1 we can note a limited variability in irradiance in winter and autumn, but a very high variability in summer.

These intra-day variabilities for a fixed day-type suggest that a careful description of the renewable energy production process must account not only for the day-type and the hour of the day, but also for the possibility of variations in irradiance within the day-type at a given hour. The histograms for the different seasons and day-types are reported in Figure 6, and examples of histograms for specific time slots, which refer to 12 noon in winter and summer, are reported in Figure 7. These histograms provide the probabilities that a given amount of energy is generated at noon in winter and summer (similar histograms provide the equivalent data for other times, as well as for spring and autumn) in the various day-types.

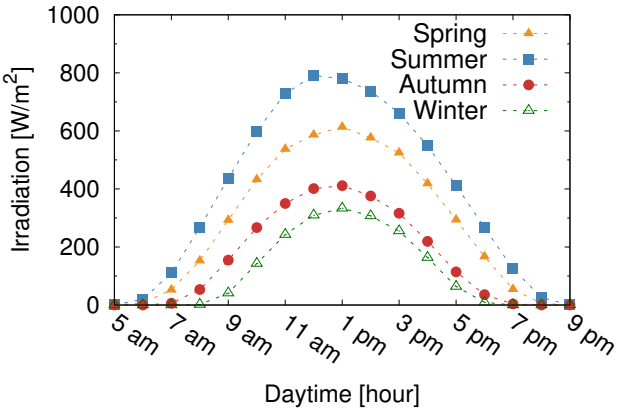

Fig. 3: Average daily irradiance per season.

III. Markov Reward Model

We define a discrete-time Markov chain (DTMC) reward model for each season S, $\mathcal{Z}^{(S)} = \{\bar{z}_n^{(S)} : n = 0, 1, \cdots\}$, over time slots of duration ΔT, set to 1 h in accordance to the time granularity of our data about solar irradiance and traffic and to the findings in [12]. For ease of notation, in what follows we focus on the description of the DTMC for a given season, and we drop the index S. However, even if not explicitly indicated, the model parameter values depend on season. The DTMC state is defined by three variables:

$$\bar{z}_n = (W_n, T_n, L_n),$$

where W_n indicates the day-type at step n; T_n represents the time of the day at step n, and L_n corresponds to the level of solar irradiance at time T_n. The battery charge level is captured

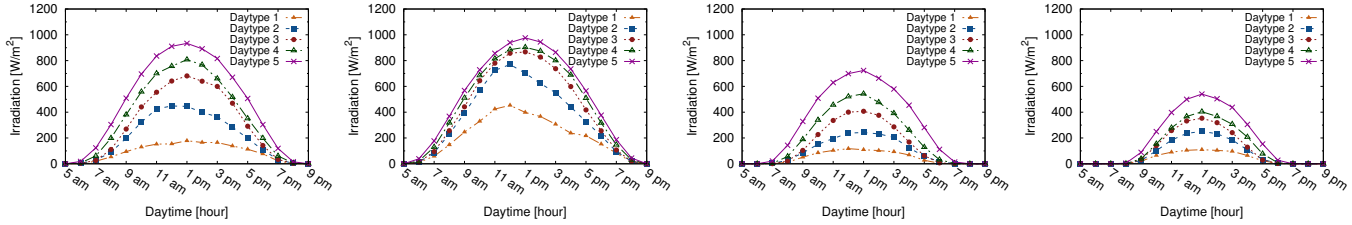

(a) Spring (b) Summer (c) Autumn (d) Winter

Fig. 4: Average daytype profiles of solar irradiance per season.

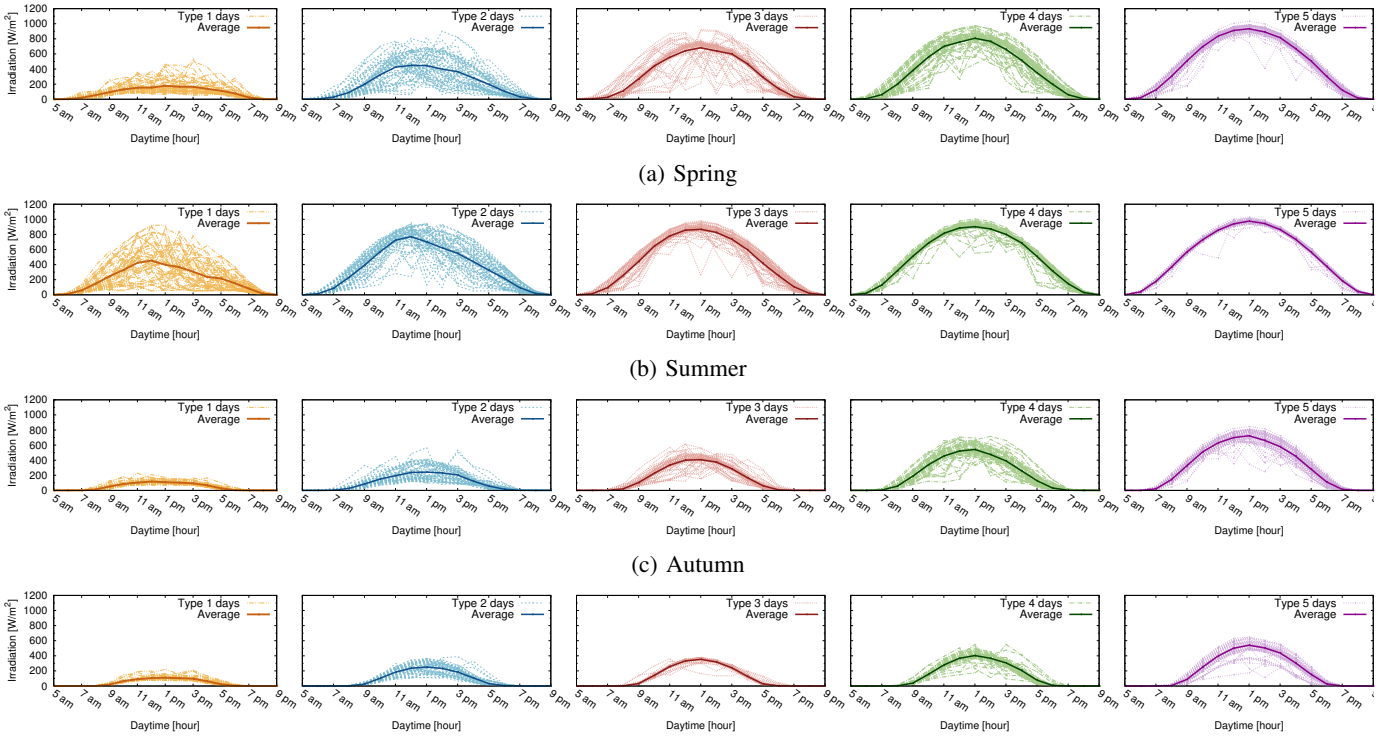

(a) Spring

(b) Summer

(c) Autumn

(d) Winter

Fig. 5: Daily profiles of solar irradiance.

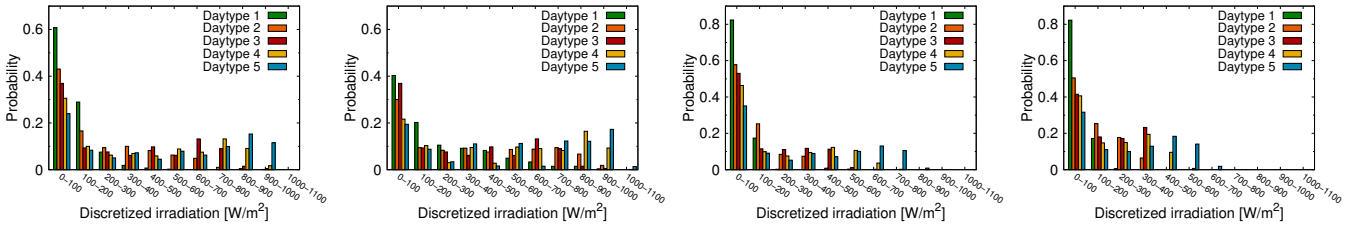

(a) Spring (b) Summer (c) Autumn (d) Winter

Fig. 6: Probability density function of solar irradiance per season.

by an accumulated reward random variable, namely B_n at step n. Roughly speaking, in each state the reward varies according to the amount of energy drained from or stored in the battery. This amount depends on the produced energy that is a random variable that, in its turn, depends on the state $\bar{z}_n$.

The DTMC moves from state $\bar{z}_n = (W_n, T_n, L_n)$ to state $\bar{z}_{n+1} = (W_{n+1}, T_{n+1}, L_{n+1})$ according to the following rules.

Flow of time: The daily evolution of the system is organized into 24 slots, corresponding to the hours of a day:

$$T_{n+1} = (T_n + 1) \mod 24 \tag{3}$$

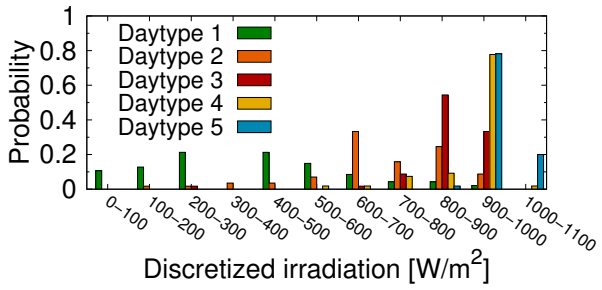

(a) Summer

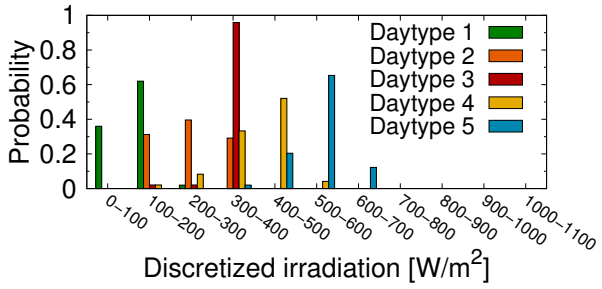

(b) Winter

Fig. 7: Probability density function of solar irradiance at 12 a.m. in Summer and Winter.

Day-type variation: The day-type changes at the end of the day according to the statistics derived from the long-term data about the daily irradiance, as described in Section II:

$$W_{n+1} = \begin{cases} W_n & \text{with pr. 1} \quad \text{if } 0 \leq T < 23 \\ W_{n+1} & \text{with pr. } P\{W_{n+1}|W_n\} \quad \text{if } T = 23 \end{cases} \tag{4}$$

where $P\{W_{n+1}|W_n\}$ is the probability that after a day of type W_n a day of type W_{n+1} follows, computed as described in the previous section.

Irradiance: The irradiance value at step n, L_n, is a random variable characterized by the day-type and the histograms for each season, day-type, and time of the day, can be computed from short-term irradiance data, which are quantized over $N_L^{(S)}$ equal size levels. The probability that the irradiance is equal to one of the possible values of L_n depends on the day-type W_n and the time of the day T_n, according to the statistics obtained from the short-term irradiance:

$$L_n = f(W_n, T_n) \tag{5}$$

This means that including L_n in the DTMC state definition is not necessary, but convenient for the computation of rewards.

Finally, the battery charge level is a continuous random variable represented by the accumulated reward; the reward gained when the DTMC visits state $\bar{z}_n$ is $r(\bar{z}_n)$. The reward $r(\bar{z}_n)$ depends on three variables:

- $E(\bar{z}_n)$: the amount of energy that is produced by the PV panel in state $\bar{z}_n$; this amount depends only on the panel size and on L_n; it is given by αL_n, where α is a constant that describes the efficiency of the PV panel;
- $C(\bar{z}_n)$: the amount of energy that is consumed by the BS in state $\bar{z}_n$, which depends only on the time of the day T_n and on the considered traffic profile (residential or business);
- $A(\bar{z}_n)$: the amount of energy that is acquired from the power grid in state $\bar{z}_n$; this amount depends on the energy purchasing policy.

The reward is expressed as:

$$r(\bar{z}_n) = E(\bar{z}_n) - C(\bar{z}_n) + A(\bar{z}_n). \tag{6}$$

The battery charging and discharging process is captured by the evolution of the cumulative reward B, given by:

$$B_{n+1} = \begin{cases} 0 & \text{if} \quad B_n + r(\bar{z}_n) \leq 0 \\ B_{\max} & \text{if} \quad B_n + r(\bar{z}_n) \geq B_{\max} \\ B_n + r(\bar{z}_n) & \text{otherwise} \end{cases} \tag{7}$$

where we account for the fact that the battery charge cannot be negative, and cannot exceed the battery capacity $B_{\max}$.

A. Reward Model Solution

The system model we just described belongs to the class of Markov-modulated fluid flow models with finite buffer, for which a variety of methods have been derived to obtain the buffer occupancy steady-state distribution. Some of them rely on solving partial differential equations (for instance, [15]). However, those solutions are fraught with problems of accuracy and efficiency, once numerical solutions of differential equations or spectral methods are used to compute performance measures.

A different set of solution approaches, developed by Ramaswami and his colleagues [16], [17], is based on the observation that the steady-state distribution of Markovian fluid flow models can be obtained from a quasi birth and death (QBD) queue. The connection to a QBD reduces the solution of a fluid model to the analysis of a discrete-time, discrete-state space QBD for which well-tested stable algorithms exist that avoid the computational difficulties arising in spectral methods. In this work, we apply the numerical method presented in [17], since we deal with the steady-state analysis of the charge in a finite-capacity battery[1].

The numerical solution method introduced by Ramaswami et al. in [17] creates coupled queues on a common probability space, by using a sequence of "spatial uniformizations", rather than the usual "time uniformization" technique [18]. The main idea of the approach is to define a discretization of the time axis, through a Markovian point process such that, in the inter-event intervals of that process, the potential increments to the flow process are identically distributed exponential random variables. Then, the fluid level is approximated by a number of exponentially distributed chunks, and a queuing model that can be represented with a QBD process is obtained. By letting the parameter of the uniformization process define progressively finer discretizations, the fluid process is obtained

[1]The implementation of the method was kindly provided to the authors by V. Ramaswami.

as the stochastic process limit of the work in the queues generated in the solution. Once the original fluid process is "reduced" to a QBD process, matrix-geometric analysis can be applied to characterize the steady-state characteristics of the fluid flow process. We refer the interested reader to the original paper [17] to get further details about the numerical method.

B. Performance Measures

From the steady-state distribution of the DTMC reward model for a given season S, with the steady-state probability to be in state $\bar{z}$ denoted by $\pi^{(S)}(\bar{z})$, we can evaluate useful performance metrics.

By computing the steady-state probability distribution of the battery charge level at the battery bounds 0 ($P[B = 0]$) and $B_{\max}$ ($P[B = B_{\max}]$), using the method in [17], we can derive:

- $P_e^{(S)}$, the empty battery probability in season S:

$$P_e^{(S)} = \sum_{\forall W} \sum_{\forall T} \sum_{\forall L} P[B = 0 | \bar{z} = (W, T, L)] \pi^{(S)}(\bar{z})$$

  When the battery is empty and no energy is produced, some brown energy has to be taken from the grid to power the BS.
- $P_f^{(S)}$, the full battery probability in season S:

$$P_f^{(S)} = \sum_{\forall W} \sum_{\forall T} \sum_{\forall L} P[B = B_{\max} | \bar{z} = (W, T, L)] \pi^{(S)}(\bar{z})$$

  When the battery is full, some possible extra-generation of green energy cannot be stored and, hence, it is wasted.

IV. Numerical Results

As already mentioned, we consider one macro BS with 2 transceivers, adopting the technology forecast for 2020 BS models [10] with the corresponding energy consumption. We consider the traffic profiles presented in Figure 2, in both the residential and business week-day versions, and we assume energy losses of 15% at both the battery input and output.

The numerical results report the values of empty battery probability, P_e, and full battery probability, P_f, for the four seasons, for the residential and business traffic profiles, and for the following three policies for brown energy acquisition.

Only-battery policy. Brown energy is acquired only when green energy is not available to run the BS, from neither the PV panel nor the battery. The amount of energy acquired from the power grid, $A(\bar{z}_n)$, used in (6) is given by:

$$A(\bar{z}_n) = \begin{cases} C(\bar{z}_n) - E(\bar{z}_n) - B_{n-1} & \text{if } C(\bar{z}_n) - E(\bar{z}_n) - B_{n-1} > 0 \\ & \text{for } 0 \leq T_n \leq 23 \end{cases}$$

Night-consumption policy. Brown energy is acquired from the grid, in the interval from midnight to 6 am, in a quantity equal to what necessary to run the base station, so that no energy is drained from the battery in this period; note that in this period energy prices are lowest; in addition, brown energy is acquired also in other periods of the day whenever green energy is not available to run the BS, from neither the PV panel nor the battery;

$$A(\bar{z}_n) = \begin{cases} C(\bar{z}_n) - E(\bar{z}_n) - B_{n-1} & \text{if } C(\bar{z}_n) - E(\bar{z}_n) - B_{n-1} > 0 \\ & \text{and if } 7 \leq T_n \leq 23 \\ C(\bar{z}_n) & \text{if } 0 \leq T_n \leq 6 \end{cases}$$

Night-consumption-and-recharge policy. Brown energy is acquired from the grid, in the interval from midnight to 6 am, in a quantity equal to what necessary to run the base station plus 1 kWh per hour, so that in this period the battery level grows of 7 kWh; as before, brown energy is acquired also in other periods of the day when green energy is not available to run the BS, from neither the PV panel nor the battery;

$$A(\bar{z}_n) = \begin{cases} C(\bar{z}_n) - E(\bar{z}_n) - B_{n-1} & \text{if } C(\bar{z}_n) - E(\bar{z}_n) - B_{n-1} > 0 \\ & \text{and if } 7 \leq T_n \leq 23 \\ C(\bar{z}_n) + 1 & \text{if } 0 \leq T_n \leq 6 \end{cases}$$

We consider three values for the PV panel size: 1, 2 and 5 kWp, and three battery capacities: 10, 15 and 20 kWh. As already noted, these PV panel sizes correspond to about 5, 10, and 25 square meters, and the battery capacities correspond to about 3, 5 and 7 car batteries (considering 12 V, 120 Ah, lead-acid batteries).

Results are reported in Figures 8, 9, 10, and 11. Plots (a), (b) and (c) refer to the residential traffic profile, while plots (d), (e) and (f) report the business area case. The red/orange/yellow bars in the figures report empty battery probabilities, while the blue/green bars report full battery probabilities. An ideal system configuration should have small empty battery probability, so that little brown energy must be acquired from the grid, and a full battery probability not too close to 1, in order to avoid wasting the green energy produced by the PV panel.

Let us start by analyzing Figure 8, that reports results referring to the spring period. As expected, by increasing the PV panel size, the probability that the battery is empty decreases while the probability that the battery is full grows.

A small PV panel of 1 kWp is not enough to guarantee a small empty battery probability, meaning that, frequently, brown energy from the grid must be purchased.

The opposite happens with a PV panel of 5 kWp: the battery is often full and rarely discharged. When some energy is taken from the grid during night (with the night-consumption and night-consumption-and-recharge policies) the empty battery probability becomes negligible, meaning that brown energy is never purchased when it is expensive.

The case of a 2 kWp PV panel has an intermediate performance. Buying the amount of brown energy that is needed for running the BS during night (night-consumption policy) is not enough, the battery discharges and some additional brown energy is needed during day time, when it is expensive.

Similar conclusions can be drawn from the summer season, whose results are reported in Figure 9. In this case, due to

the higher irradiance, reducing the empty battery probability is even easier than in spring. With a PV panel of 2 kWp, the system is almost autonomous from the power grid: the empty battery probability is below few percentage points for medium-size batteries even under the only-battery policy.

By comparing the cases of the residential and the business profiles, we observe that performance is very similar. There are indeed two major differences between the profiles whose effects somehow balance. On the one side, the fact that the business profile is more correlated with solar production (i.e., the peak traffic occurs during high energy production periods) makes the system more autonomous from the grid and with less need to use the battery as power supply. On the other hand, the business profile has a slightly larger daily energy consumption.

Let us now turn our attention to Figure 10 that reports the autumn case. Since the irradiance is much smaller than in spring or summer, the only-battery and night-consumption policies cannot provide a small empty battery probability; even with a 5 kWp panel the battery is frequently discharged and rarely full. The battery regularly fills only under the night-consumption-and-recharge policy. In winter this phenomenon is further noticeable, as shown in Figure 11. A PV panel of 2 kWp provides good performance only under the night-consumption-and-recharge policy, while unacceptable values of the empty battery probability are achieved under the other two policies.

Two main conclusions can be drawn from these results. First, in order to optimize the use of an hybrid PV/grid power supply system, a smart energy management strategy should adopt policies that change based on the season. While in summer, the power supply system can rely uniquely on the battery, in winter a preventive brown energy purchase during low price periods (i.e., during night) is convenient. Second, with a smart energy management strategy even small PV panels, of about 10 square meters, and few batteries are enough for a green BS operation. This makes the deployability of green BSs much easier, even in urban environments, a very interesting conclusion in view of the network densification that is expected for the next years.

V. Related Work

The increasing number and variety of works available in the literature about green mobile networks shows the raising interest about the use of RE to make communication networks more energy efficient [19]–[21].

Most related with this paper are the works that aim at modeling the behavior of BS power systems based on renewables, with the objective of understanding the characteristics of these systems and providing guidelines for correct dimensioning [12], [22]–[24]. Those works rely on Markovian models for computing BSs performance, in which battery charge levels are explicitly modeled as one of the Markov chain state-variables. To the best of our knowledge, this work is the first one that applies Markov reward models for dimensioning both panel and battery sizes of BS renewable power systems. Applying reward technique to describe the battery charge as a continuous variable enables a more accurate performance evaluation of a BS system, given that previous studies showed that battery modeling is the most critical system element as regards quantization [12].

VI. Conclusions

In this paper, we consider a base station that, besides being connected to the power grid, is equipped with a solar panel and an energy storage unit. By modeling the system as a Markov reward process, we investigate three energy management strategies: i) brown energy is drained from the grid only when the battery is discharged, ii) the base station is powered through brown energy from the grid also during night, when the price of electricity is low, and, iii) during night, in addition to the energy needed to run the BS, some brown energy is preventively stored in the battery for future usage.

The results show that the effectiveness of the policies strongly depends on the season. Hence, a smart energy management strategy should alternate the considered policies. With such a strategy, even small PV panels of about 10 square meters are enough to effectively reduce operational costs and carbon footprint. The possibility to use limited size panels is very attractive for network operators that are interested in reducing the operational cost of the access network, while having to cope with the need for network densification.

References

[1] M. Gupta and S. Singh, "Greening of the internet," in *Proceedings of the 2003 Conference on Applications, Technologies, Architectures, and Protocols for Computer Communications*, ser. SIGCOMM '03. New York, NY, USA: ACM, 2003, pp. 19–26. [Online]. Available: http://doi.acm.org/10.1145/863955.863959

[2] D. Zeller, M. Olsson, O. Blume, A. Fehske, D. Ferling, W. Tomaselli, and I. Gódor, *Sustainable Wireless Broadband Access to the Future Internet - The EARTH Project*. Berlin, Heidelberg: Springer Berlin Heidelberg, 2013, pp. 249–271.

[3] R. Bolla, R. Bruschi, F. Davoli, L. D. Gregorio, L. Giacomello, C. Lombardo, G. Parladori, N. Strugo, and A. Zafeiropoulos, "The low energy consumption networks (econet) project," in *2012 Second IFIP Conference on Sustainable Internet and ICT for Sustainability (SustainIT 2012)(SUSTAINIT)*, vol. 00, Oct. 2013, pp. 1–5. [Online]. Available: doi.ieeecomputersociety.org/

[4] M. Ajmone Marsan, C. Guerrero, S. Buzzi, F. Idzikowski, L. Chiaraviglio, M. Meo, Y. Ye, and J. L. Vizcaíno, "TREND: toward real energy-efficient network design," in *Sustainable Internet and ICT for Sustainability, SustainIT 2012, 4-5 October, 2012, Pisa, Italy, Sponsored by the IFIP TC6 WG 6.3 "Performance of Communication Systems"*, 2012, pp. 1–6. [Online]. Available: http://ieeexplore.ieee.org/document/6388030/

[5] GreenTouch Consortium, 2015. [Online]. Available: https://s3-us-west-2.amazonaws.com/belllabs-microsite-greentouch/index.php@page=about-us.html

[6] Z. Hasan, H. Boostanimehr, and V. K. Bhargava, "Green cellular networks: A survey, some research issues and challenges," *Communications Surveys Tutorials, IEEE*, vol. 13, pp. 524 – 540, 08 2011.

[7] A. D. Domenico, E. C. Strinati, and A. Capone, "Enabling green cellular networks: A survey and outlook," *Computer Communications*, vol. 37, pp. 5 – 24, 2014. [Online]. Available: http://www.sciencedirect.com/science/article/pii/S0140366413002168

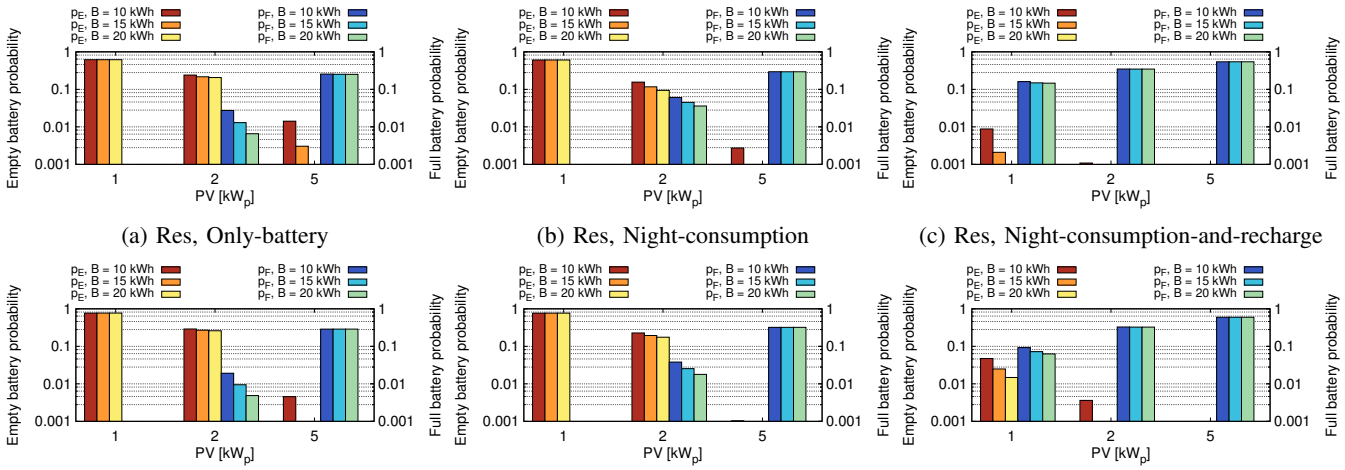

(a) Res, Only-battery (b) Res, Night-consumption (c) Res, Night-consumption-and-recharge

(d) Bus, Only-battery (e) Bus, Night-consumption (f) Bus, Night-consumption-and-recharge

Fig. 8: Empty battery probability and full battery probability in **spring**, under different energy management strategies, in the Residential and Business areas.

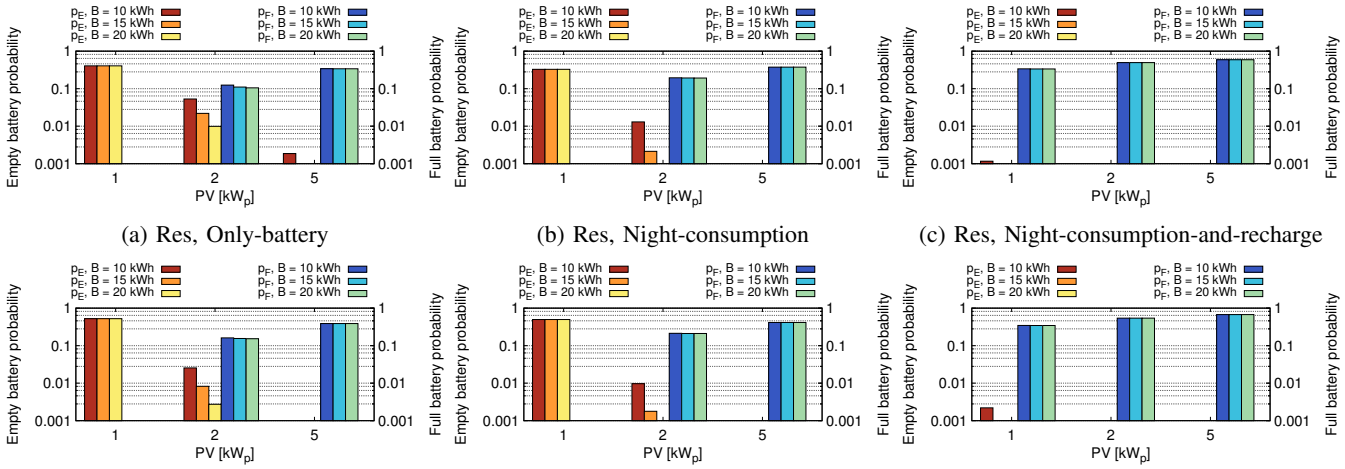

(a) Res, Only-battery (b) Res, Night-consumption (c) Res, Night-consumption-and-recharge

(d) Bus, Only-battery (e) Bus, Night-consumption (f) Bus, Night-consumption-and-recharge

Fig. 9: Empty battery probability and full battery probability in **summer**, under different energy management strategies, in the Residential and Business areas.

[8] ukasz Budzisz, F. Ganji, G. Rizzo, M. A. Marsan, M. Meo, Y. Zhang, R. Tassiulas, S. Lambert, B. Lannoo, M. Pickavet, A. Conte, I. Haratcherev, and A. Wolisz, "Dynamic resource provisioning for energy efficiency in wireless access networks: A survey and an outlook," *Commun. Surv. Tutor. IEEE 2014*, pp. 2259–2285.

[9] Disclosure Inside Act, 2010. [Online]. Available: https://www.cdp.net/zh/articles/climate/case-study-china-mobile

[10] F. L. Bjorn Debaillie, Claude Desset, "A flexible and future-proof power model for cellular base stations," in *81st IEEE Vehicular Technology Conference*. IEEE, 2015.

[11] M. Meo, Y. Zhang, R. Gerboni, and M. A. Marsan, "Dimensioning the power supply of a LTE macro BS connected to a PV panel and the power grid," in *2015 IEEE International Conference on Communications, ICC 2015, London, United Kingdom, June 8-12, 2015*, 2015, pp. 178–184. [Online]. Available: http://dx.doi.org/10.1109/ICC.2015.7248318

[12] A. P. C. da Silva, D. Renga, M. Meo, and M. Ajmone Marsan, "The impact of quantization on the design of solar power systems for cellular base stations," *IEEE Transactions on Green Communications and Networking*, vol. 2, no. 1, pp. 260–274, 2018.

[13] Y. Zhang, L. Budzisz, M. Meo, A. Conte, I. Haratcherev, G. Koutitas, L. Tassiulas, M. Ajmone Marsan, and S. Lambert, "An overview of energy-efficient base station management techniques," in *Proc. of TIWDC'13 (24th Tyrrhenian Int. Workshop on Digital Communications)*, September 2013, ConferenceProceedings.

[14] SODA (Solar radiation Data), "Solar Energy Services for Professionals," 2014. [Online]. Available: http://www.soda-pro.com/

[15] D. Anick, D. Mitra, and M. Mohan Sondhi, "Stochastic theory of a data-handling system with multiple sources," *Bell System Technical Journal*, vol. 61, 10 1982.

[16] S. Ahn and V. Ramaswami, "Fluid flow models and queuesa connection by stochastic coupling," *Stochastic Models, doi = 10.1081/STM-120023564*, vol. 19, 08 2003.

[17] ——, "Steady State Analysis of Finite Fluid Flow Models Using Finit QBDs," *Queueing Systems*, no. 49, pp. 223–259, 2005.

[18] A. Jensen, "Markoff chains as an aid in the study of markoff processes," *Skandinavsk Aktuarietidskrift*, vol. 36, pp. 87–91, 1953.

[19] D. Renga, H. A. H. Hassan, M. Meo, and L. Nuaymi, "Improving the interaction of a green mobile network with the smart grid," in *2017 IEEE International Conference on Communications (ICC)*, May 2017, pp. 1–7.

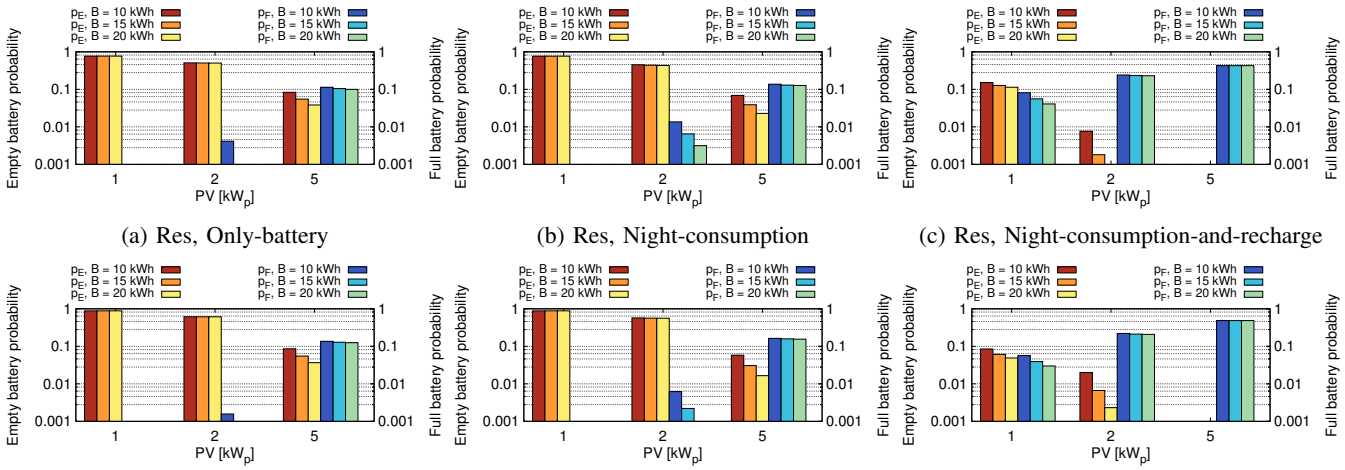

(a) Res, Only-battery (b) Res, Night-consumption (c) Res, Night-consumption-and-recharge

(d) Bus, Only-battery (e) Bus, Night-consumption (f) Bus, Night-consumption-and-recharge

Fig. 10: Empty battery probability and full battery probability in **autumn**, under different energy management strategies, in the Residential and Business areas.

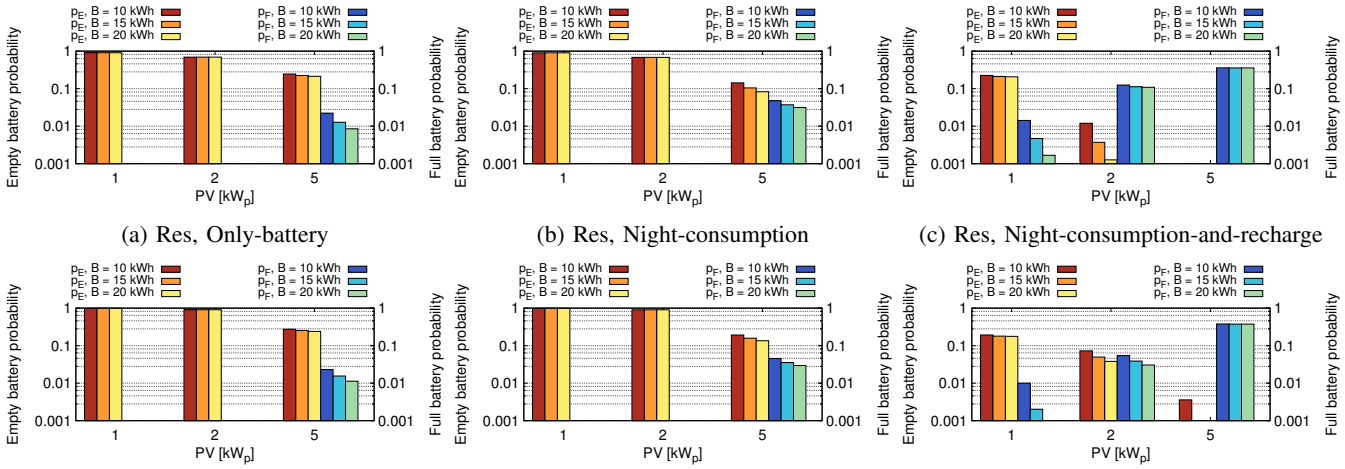

(a) Res, Only-battery (b) Res, Night-consumption (c) Res, Night-consumption-and-recharge

(d) Bus, Only-battery (e) Bus, Night-consumption (f) Bus, Night-consumption-and-recharge

Fig. 11: Empty battery probability and full battery probability in **winter**, under different energy management strategies, in the Residential and Business areas.

[20] M. Ali, M. Meo, and D. Renga, *Cost Saving and Ancillary Service Provisioning in Green Mobile Networks: Technology, Communications and Computing*, 01 2019, pp. 201–224.

[21] M. H. Alsharif, J. Kim, and J. H. Kim, "Green and sustainable cellular base stations: An overview and future research directions," *Energies*, vol. 10, no. 5, 2017.

[22] V. Chamola and B. Sikdar, "Outage estimation for solar powered cellular base stations," in *ICC*. IEEE, 2015, pp. 172–177.

[23] J. Song, V. Krishnamurthy, A. Kwasinski, and R. Sharma, "Development of a markov-chain-based energy storage model for power supply availability assessment of photovoltaic generation plants," *IEEE Transactions on Sustainable Energy*, vol. 4, no. 2, pp. 491–500, April 2013.

[24] G. Leonardi, M. Meo, and M. A. Marsan, "Markovian models of solar power supply for a LTE macro BS," in *2016 IEEE International Conference on Communications, ICC 2016, Kuala Lumpur, Malaysia, May 22-27, 2016*, 2016, pp. 1–7. [Online]. Available: http://dx.doi.org/10.1109/ICC.2016.7510698